

# **DETRITAL COSMOCHRONOLOGY OF THE GREENLAND ICE SHEET**

A thesis proposal presented by

Lee Corbett

To the faculty of the Geology Department of the University of Vermont

May 2008

Accepted by the faculty of the University of Vermont, in partial fulfillment of the requirements for the degree of Masters of Science specializing in Geology.

The following members of the Thesis Committee have read and approved this document:

Advisor, Paul Bierman: \_\_\_\_\_

Advisor, Tom Neumann: \_\_\_\_\_

Chair, Shelly Rayback: \_\_\_\_\_

## I. INTRODUCTION

The size of the Greenland Ice Sheet has not been stable over time; instead, it has varied substantially with periods of warm and cool climate (e.g. Nishiizumi et al., 1996; Letréguilly et al., 1991; Cuffey and Marshall, 2000; Otto-Bliesner et al., 2006). Understanding this dynamic system is especially important today, as the Greenland Ice Sheet will likely have a significant melting response to anthropogenic climate change (e.g. Huybrechts et al., 1991; Alley et al., 2005; Gregory et al., 2004). By determining how the ice sheet has reacted to past climate changes during the Quaternary, we will be better able to anticipate its reaction to climate changes in the present and the future.

This project will use a technique called *cosmogenic burial dating* (e.g. Granger and Muzikar, 2001) to assess times when the ice sheet was smaller than it is today. The measurement of terrestrial cosmogenic nuclides ( $^{10}\text{Be}$ ,  $^{26}\text{Al}$ ,  $^{36}\text{Cl}$ , and  $^{14}\text{C}$ ) in clasts gathered from the ice sheet margin will allow calculation of the amount of time since the clasts were last exposed to cosmic radiation. Using this technique at several different field sites will help to constrain the geographic extent of past ice-melting events.

The goals of this project are threefold: first, to further develop the burial dating technique and apply it within the scope of this project; second, to infer information about ice sheet history by sampling clasts from three locations at the ice sheet margin; and third, to use this information to predict how modern warming might impact changes in the geographic extent of the ice sheet.

## II. STUDY SITE

The Greenland Ice Sheet occupies about  $1.7 \times 10^6 \text{ km}^2$  of land area and is the second largest ice sheet in the world after the Antarctic Ice Sheet. It covers 81% of Greenland, with the unglaciated areas found predominately around the coast and in the southwestern region.

Although the thickness of the ice sheet near the coast is only 10's of meters, it grows to roughly 3,400 m at the center (Huybrechts et al., 1991). Because of Greenland's polar climate, the ice sheet is frozen to the bed in most locations and only reaches the pressure melting point in the areas of thickest ice and in the relatively warm coastal regions (Huybrechts, 1995). Greenland

has been at least partially glaciated since about 7 Ma, although continuous ice cover did not develop until the late Pliocene (Larsen et al., 1994). The bedrock geology of Greenland is complex and includes an abundance of Precambrian crystalline rocks, chiefly granites and gneisses (Escher and Pulvertaft, 1995).

This study will investigate three different sites along the western coast of Greenland (fig. 1). The southernmost site, Kangerlussuaq, is just above the Arctic Circle at 67°00'38'' N and lies at the head of one of the largest fjords in Greenland, Søndre Strømfjord. At Kangerlussuaq the ice margin is far from the coast and this region is believed to have been significantly or completely deglaciated during the last interglacial period (e.g. Cuffey and Marshall, 2000). The middle site, Ilulissat, hosts the third largest settlement in Greenland and is located at 69°13'00'' N. It is in close proximity to the famous Jakobshavn Isbræ glacier, the most productive calving glacier in the northern hemisphere, and sits directly on the iceberg-choked Ilulissat Fjord. The ice margin here is relatively close to the coast. The northernmost site, Upernavik, is at 72°47'02'' N. The settlement of Upernavik sits on a currently unglaciated offshore island, as the ice sheet on the mainland extends almost completely to the sea. Detailed studies performed at the ice margin near Kangerlussuaq and Ilulissat suggest that there is abundant debris entrained in the ice, an ideal set of conditions for this project (Knight et al., 2002; Sugden et al., 1987). Less work has been done in the area near Upernavik and the conditions of the ice sheet are not well known.

### **III. CLIMATE AND THE GREENLAND ICE SHEET**

#### **3.1. History of the Greenland Ice Sheet**

The Greenland Ice Sheet is a large feature with important impacts on global climate and sea level. Unfortunately, though, the age of its initial formation is poorly constrained. The oldest widespread ice rafted debris (IRD) found in North Atlantic deep sea cores dates back to around 2.4 Ma (e.g. Shackleton et al., 1984), and small amounts of IRD off the coast of Norway are as old as 5.4 Ma (Jansen et al., 1990). Relatively recent work off the southeast coast of Greenland indicates that the first ice-transported dropstones occurred in the Late Miocene, roughly 7 Ma (Larsen et al., 1994). These dates, however, do not necessarily represent the actual onset of northern hemisphere glaciation because IRD is only produced when glaciers or ice sheets

become large enough to reach the sea. Larsen et al. (1994) suggest that glaciation actually began much earlier, likely at the onset of cooling in the early Late Miocene around 10 Ma. Full glacial conditions would have been established by about the middle Late Miocene (7 Ma), allowing glaciers in Greenland to reach the sea, calve icebergs, and contribute to the deposition of IRD in the deep sea sediments.

If the Greenland Ice Sheet had reached its full extent roughly 7 Ma, then how much of the subsequent time has the ice sheet stayed at that size? The answer to this question is also poorly understood, although this research will attempt to clarify the behavior of the ice sheet over the past several hundred ka. Nishiizumi et al. (1996) found evidence of cosmic ray exposure in the rocks below the Greenland Ice Sheet Project 2 (GISP2) ice core, suggesting that Greenland's summit was fully deglaciated for several thousand years around 0.5 +/- 0.2 Ma. If this data is robust, then much, if not all, of the present-day Greenland Ice Sheet is many times younger than was originally thought. This melting episode could be correlated with marine oxygen isotope stage (OIS) 11, one of many stages of minimum global ice volume inferred from benthic foraminifera oxygen isotope reconstructions from deep sea sediment cores (Lisiecki and Raymo, 2005).

There is also substantial evidence that the ice sheet was smaller during the last interglacial period, the Eemian (~130 ka), which equates to marine OIS stage 5. Modeling efforts by Letréguilly et al. (1991), Cuffey and Marshall (2000), Overpeck et al. (2006), and Otto-Bliesner et al. (2006) suggest that the Greenland Ice Sheet may have melted significantly, therefore accounting for the large volume of sea level rise observed in paleoclimate records of the Eemian. Models suggest that, for the most part, this melting would have occurred around the coast and in the southwestern region near Kangerlussuaq, leaving intact ice in the center of Greenland and possibly in the southern highlands (figs. 2a and 2b).

As described above, evidence suggests that the Greenland Ice Sheet may have melted partially or completely during OIS 5 and 11. During the Quaternary, however, there were four other interglacial periods with equally low global ice volumes: OIS 9, 25, 31, and 47 (Lisiecki and Raymo, 2005) (fig. 3). Thus, it is reasonable to believe that the ice sheet may have undergone significant melting episodes during these times as well, suggesting that the ice sheet is a dynamic system that actively changes with climate.

In more recent times, the Greenland Ice Sheet was again extensive during the last glacial maximum (LGM) of the latest Pleistocene (~23 ka). At the height of the LGM, it is thought that the entire continent of Greenland, plus much of the surrounding continental shelf, was glaciated (Bennike and Bjorck, 2002). The last deglaciation chronology is complicated, with ice melting first on the southern peninsula (~14 ka) and latest on the northern tip (possibly as recent as ~9 ka) with substantial local variability between the two extremes (e.g. Bennike and Bjorck, 2002; Håkansson et al., 2007). The ice sheet then reached its minimum Holocene extent during the Holocene Climatic Optimum ~5 ka, and from that time grew until the termination of the Little Ice Age ~1850 (Weidick et al., 1990). Recent work has suggested thinning, retreat, and increased flow velocity of Greenland's outlet glaciers over the past several decades (e.g. Joughin et al., 2004).

### **3.2. Future of the Greenland Ice Sheet**

Overpeck et al. (2006) and Cuffey and Marshall (2000) demonstrate through modeling that melting of the Greenland Ice Sheet can have significant implications for global sea level. The ice sheet contains a volume of about  $2.8 \times 10^6 \text{ km}^3$  of ice (Huybrechts et al., 1991) and full melting of the ice sheet could contribute 6-7 meters of sea level rise (Alley et al., 2005), which would submerge many of the world's heavily populated coastal cities. Although there is still uncertainty surrounding how much greenhouse gas concentrations and global temperature will rise during the next centuries (IPCC, 2007), it is possible that the ice sheet could undergo significant melting in the near future, resulting in the disappearance of the ice sheet entirely on the timescale of several millennia (e.g. Gregory et al., 2004, Overpeck et al., 2006).

## **IV. COSMOGENIC DATING**

### **4.1. Cosmogenic Dating Theory and Cosmogenic Exposure Dating**

The basis of cosmogenic dating is a process that involves bombardment of terrestrial material by two types of cosmic particles: nucleons and muons (e.g. Granger and Muzikar, 2001). These high-energy cosmic particles cause the formation of about two-dozen different isotopes that are not produced by any other common mechanism (Lal, 1988; Sharma and

Middleton, 1989). The most frequently used isotopes for dating purposes include  $^3\text{He}$ ,  $^{21}\text{Ne}$ ,  $^{10}\text{Be}$ ,  $^{26}\text{Al}$ ,  $^{36}\text{Cl}$ , and  $^{14}\text{C}$ . The first two are stable noble gases, while the latter four are solid phase radionuclides listed by decreasing half-life (1.3 Ma, 0.7 Ma, 0.3 Ma, and 5.7 ka respectively) (Gosse, 2007; Nishiizumi et al., 2007).

Cosmogenic nuclide dating is based on the assumption that terrestrial cosmogenic nuclides (TCNs) are formed through bombardment of rock surfaces by cosmogenic particles at known rates, although these rates vary spatially as a function of geomagnetic field strength and altitude (Lal, 1991). According to work done by Nishiizumi et al. (1989), the estimated production rate for  $^{10}\text{Be}$  at sea level above  $50^\circ\text{N}$ , due to both nucleons and muons, is 6.03 atoms per gram of quartz per year. The production rate for  $^{26}\text{Al}$ , assuming the same set of conditions, is estimated at 36.8 atoms per gram of quartz per year. More recent work by Gosse and Stone (2001) suggests that  $^{10}\text{Be}$  production is lower, only about 5.2 atoms per gram of quartz per year. For the purposes of this study, production rates of 5.2 (for  $^{10}\text{Be}$ ) and 31.2 (for  $^{26}\text{Al}$ ) atoms per gram of quartz per year at the surface of the rock will be used. Knowing the TCN concentration in a sample as well as the production rate of that particular TCN allows inferences to be made about a sample's exposure history to cosmic radiation.

The traditional form of cosmogenic dating, called exposure dating, is concerned with determining how recently a surface (e.g. a boulder on a glacial moraine) was exposed. Assuming that the boulder had no TCNs leftover from previous periods of exposure and has not eroded since exposure, measuring the abundance of TCNs in the sample would therefore indicate how long that bedrock surface has been uncovered and subjected to bombardment by cosmogenic particles (e.g. Munroe et al., 2006). If using a radioactive TCN, the rate of decay must also be taken into account as well. This application of cosmogenic dating is relatively straightforward and can be performed with a single nuclide, frequently  $^{10}\text{Be}$ .

#### **4.2. Cosmogenic Burial Dating**

In Greenland, cosmogenic exposure dating has been used to constrain the extent of the ice sheet during the last glacial maximum (Håkansson et al., 2007). In the case of this study, however, exposure dating will not answer questions about past periods of melting because the once ice-free areas have since been re-covered with ice. A related technique, called cosmogenic burial dating, must therefore be used (e.g. Granger and Muzikar, 2001). Cosmogenic burial

dating relies on the principle that radioactive TCNs are formed at a known rate and decay at another known rate. If two TCNs are used, the ratio of their concentrations can be correlated to the amount of time the surface spent exposed (thus accumulating TCNs) and the amount of time the surface spent shielded from radiation (thus decaying radioactive TCNs) (Granger and Muzikar, 2001). For example, in an area where glaciers have periodically advanced and retreated, the ratio of  $^{26}\text{Al}$  to  $^{10}\text{Be}$  can indicate what fraction of the time the bedrock was exposed versus buried by ice (e.g. Bierman et al., 1999).

Typically, two or more TCNs are used simultaneously, as described below in more detail. Assuming that a rock surface was exposed for a long duration of time, the ratio of the concentrations of the TCNs follows a curved path as shown by the dashed “constant exposure” line in figure 4. The starting point of this graph is determined by the ratio of production rates of the two TCNs (~6, in the case of  $^{26}\text{Al}/^{10}\text{Be}$ ). The path that the line follows is determined by the rate constants of the TCNs (the rate at which they decay) and the duration of exposure. Eventually, if no burial or erosion occurs, the path will reach a point of secular equilibrium where the rate of decay is equal to the rate of production.

In the simplest model of burial dating, a surface is exposed to cosmic radiation for an amount of time much shorter than the half-lives of the TCNs, and then buried deeply enough to halt all TCN production (Granger and Muzikar, 2001). In figure 4, this would equate to traveling along the curved dashed “constant exposure” line for a certain amount of time proportional to the duration of cosmic ray exposure, and then traveling perpendicularly to that path across the burial isochrones for an amount of time proportional to the duration of burial. As shown by the path described above, the  $^{26}\text{Al}/^{10}\text{Be}$  ratio decreases with burial because the half-life of  $^{26}\text{Al}$  (0.7 Ma) is shorter than that of  $^{10}\text{Be}$  (1.3 Ma).

It is unknown what type of exposure the clasts under the Greenland Ice Sheet have undergone, but it is possible that their histories are complicated due to continual advances and retreats of the ice sheet. If the clasts have undergone multiple episodes of exposure separated by periods of burial beneath the ice, the actual path of the rock in figure 4 cannot be calculated. However, the ratio of burial duration to exposure duration can be used to infer several possible paths and the most reasonable of those options can be selected. Additionally, using four TCNs ( $^{10}\text{Be}$ ,  $^{26}\text{Al}$ ,  $^{36}\text{Cl}$ , and  $^{14}\text{C}$ ) instead of two will provide further insight since different half-lives will provide wider temporal resolution.

## V. METHODS AND TIMELINE

### 5.1. Spring and Early Summer 2008: Preparation

The spring of 2008 will be spent in preparation for the field season by accomplishing the following tasks. First, we will investigate topographic maps, satellite imagery, and aerial photographs of Greenland's west coast to determine sampling locations at the three ice sheet margin sites described above. Sites will be selected based on the simplicity of ice flow patterns and accessibility. Second, we will contact researchers who have done previous work on the Greenland Ice Sheet (e.g. R. Alley, P. Knight, and others) to obtain more information about the ice sheet margin at the above locations. Third, we will make all necessary trip preparations and develop field-sampling strategies.

### 5.2. July 2008: Fieldwork

In July of 2008, we will fly to Greenland and spend 3-4 weeks sampling clasts from the ice margin. For each sample site we will perform initial reconnaissance by helicopter to ensure that the ice sheet margin is accessible and safe. We will then reach the sample site by helicopter drop or by foot and will stay there for several hours to several days for sampling.

First, we will conduct an overall survey of the ice margin at the sample site and will record observations about placement/abundance of debris inclusions, lithology of inclusions, ice quality, and other features. Second, we will extract roughly 100 clasts from the ice margin by hammer, ice axe, and/or blowtorch. Clasts will be chosen based on size, rock type, and quartz abundance, since quartz crystals are needed to perform cosmogenic nuclide dating of  $^{10}\text{Be}$  and  $^{26}\text{Al}$ . Each clast will be photographed, weighed, labeled, and securely packaged for transport from the field site.

### 5.3. Late Summer 2008 Through Winter 2009: Sample Preparation

After the field season, we will catalogue and re-evaluate clasts for cosmogenic nuclide dating suitability. The final suite of clasts (~100) will be chosen and the process of sample preparation will begin. The goal of sample preparation is to isolate enough quartz (for  $^{10}\text{Be}$ ,  $^{26}\text{Al}$ , and  $^{14}\text{C}$ ) or feldspar (for  $^{36}\text{Cl}$ ) to achieve measurable concentrations of TCNs. This will equate to roughly 100 g of quartz and 50 g of feldspar.



To isolate quartz (for the analysis of  $^{10}\text{Be}$ ,  $^{26}\text{Al}$ , and  $^{14}\text{C}$ ), the samples must be crushed and ground and the magnetic fraction must be removed. Next, dilute acid etching will purify the quartz crystals, and then mineral separation will be performed to remove quartz crystals from minerals with other densities. A final acid etching will follow, and the resulting mineral separate will be tested for purity using ICP. After quartz crystals have reached an acceptable level of purity, samples will be dissolved and treated to remove Fe and Ti, the most prevalent accessory ions in quartz aside from Be and Al. This study will use methods developed at the University of Vermont (UVM Cosmogenic Nuclide Laboratory, 2001).

To isolate feldspar (for the analysis of  $^{36}\text{Cl}$ ), methods will be used from Stone et al. (1996). After crushing, grinding, and dissolution, a series of chemical precipitations will be performed to isolate and isolate Cl from K-rich minerals.

#### **5.4. Spring 2009: Sample Analysis**

During the spring of 2009, all samples will be analyzed for  $^{10}\text{Be}$ , and then samples showing detectable  $^{10}\text{Be}$  concentrations will be analyzed for  $^{26}\text{Al}$ ,  $^{36}\text{Cl}$ , and  $^{14}\text{C}$ . This approach will be used because  $^{10}\text{Be}$  has the longest half-life and can be used as a screening tool for which samples might also contain the TCNs with shorter half-lives. We will collect data for  $^{10}\text{Be}$ ,  $^{26}\text{Al}$ , and  $^{36}\text{Cl}$  at the Lawrence Livermore National Laboratory in California, and data for  $^{14}\text{C}$  at the University of Arizona Laboratory. Samples will be run in small batches throughout the spring in order to obtain preliminary data that will be used to guide further analysis.

In addition, J. Graly will conduct computer modeling of Greenland Ice Sheet flow to determine where the clasts originated in order to better understand the geospatial aspects of ice sheet melt.

#### **5.5. Summer 2009 Through Spring 2010: Analysis, Presentation, and Writing**

Once sample analysis is complete, the next year will be spent analyzing the data in order to infer information about past ice-melting events in Greenland. This time span will also include multiple conference presentations, as well as the thesis writing and thesis defense.

## **VI. SUMMARY**

Paleoclimatic evidence of past Greenland Ice Sheet behavior, as well as modeling evidence of future Greenland Ice Sheet behavior, suggests that the system is more dynamic than was once thought. Since partial or complete melting of the ice sheet could contribute significantly to global sea level rise, it is important to understand the conditions that could contribute to melting and to estimate how long the ice sheet might stay in a melted state before beginning to grow again.

Aside from one suite of TCN measurements (Nishiizumi et al., 1996) there have been few field-based studies of past ice sheet extent. This work, therefore, will provide much needed information about how the Greenland Ice Sheet has reacted to past climate changes and how it might react to changes in the future.

## SOURCES CITED

- Alley, R.B., P.U. Clark, P. Huybrechts, and I. Joughin. 2005. Ice-sheet and sea-level changes. *Science* 310: 456-460.
- Bennike, O., and S. Bjorck. 2006. Chronology of the last recession of the Greenland Ice Sheet. *Journal of Quaternary Science* 17(3): 211-219.
- Bierman, P.R., K.A. Marsella, C. Patterson, P.T. Davis, and M. Caffee. 1999. Mid-Pleistocene cosmogenic minimum-age limits for pre-Wisconsinan glacial surfaces in southwestern Minnesota and southern Baffin Island: a multiple nuclide approach. *Geomorphology* 27: 25-39.
- Cuffey, K.M. and S.J. Marshall. 2000. Substantial contribution to sea-level rise during the last interglacial from the Greenland Ice Sheet. *Nature* 404: 591-594.
- Escher, J.C. and T.C.R. Pulvertaft. 1995. Geological Map of Greenland 1:2,500,000. Geological Survey of Greenland, Copenhagen.
- Geodetic Institute. 1938. Map of Greenland 1:4,000,000. Geodetic Institute of Copenhagen.
- Gosse, J.C. 2007. "Cosmogenic Nuclide Dating", in *Encyclopedia of Quaternary Science*, S.A. Elias ed. Elsevier Ltd.
- Gosse, J.C. and J.O. Stone. 2001. Terrestrial cosmogenic nuclide methods passing milestones toward paleo-altimetry. *EOS* 82(7): 82-89.
- Granger, D.E., and P.F. Muzikar. 2001. Dating sediment burial with in situ-produced cosmogenic nuclides: theory, techniques, and limitations. *Earth and Planetary Science Letters* 188: 269-281.
- Gregory, J.M., P. Huybrechts, and S.C.B. Raper. 2004. Threatened loss of the Greenland Ice Sheet. *Nature* 428: 616.
- Håkansson, L., J. Briner, H. Alexanderson, A. Aldahan, and G. Possnert. 2007. <sup>10</sup>Be ages from central east Greenland constrain the extent of the Greenland ice sheet during the Last Glacial Maximum. *Quaternary Science Reviews* 26: 2316-2321.
- Huybrechts, P. 1995. Basal temperature conditions of the Greenland Ice Sheet during the glacial cycles. *Annals of Glaciology* 23: 226-236.
- Huybrechts, P., A. Letreguilly, and N. Reeh. 1991. The Greenland Ice Sheet and greenhouse warming. *Paleogeography, Paleoclimatology, Paleoecology (Global and Planetary Change Section)* 89: 399-412.
- IPCC. 2007. Climate Change 2007- The Physical Science Basis. In *IPCC Fourth Assessment Report*. Cambridge University Press, Cambridge.

- Jansen, E., J. Sjöholm, U. Bleil, J.A. Erichsen. 1990. In *Geological History of the Polar Oceans: Arctic Versus Antarctic*, U. Beil and J. Thied eds., Kluwer Amsterdam.
- Joughin, I., W. Abdalti, and M. Fahnestock. 2004. Large fluctuations in speed on Greenland's Jakobshavn Isbræ. *Nature* 432: 608-610.
- Knight, P.G., R.I. Waller, C.J. Patterson, A.P. Jones, and Z.P. Robinson. 2002. Discharge of debris from ice at the margin of the Greenland Ice Sheet. *Journal of Glaciology* 48(161): 192-198.
- Lal, D. 1991. Cosmogenic ray labeling of erosion surfaces: *in situ* nuclide production rates and erosion models. *Earth and Planetary Science Letters* 104: 424-439.
- Lal, D. 1988. In situ-produced cosmogenic isotopes in terrestrial rocks. *Annual Review of Earth and Planetary Science* 16: 355-388.
- Larsen, H.C., A.D. Saunders, P.D. Clift, J. Beget, W. Wei, S. Spezzaferri. 1994. Seven million years of glaciation in Greenland. *Science* 264: 952-955.
- Letréguilly, A., N. Reeh, and P. Huybrechts. 1991. The Greenland Ice Sheet through the last glacial-interglacial cycle. *Paleogeography, Paleoclimatology, Paleoecology (Global and Planetary Change Section)* 90: 385-394.
- Lisiecki, L.E. and M.E. Raymo. 2005. A Pliocene-Pleistocene stack of 57 globally distributed benthic  $\delta^{18}\text{O}$  records. *Paleoceanography* 20: PA1003.
- Munroe, J.S., B.J.C. Laabs, J.D. Shakun, B.S. Singer, D.M. Mickelson, K.A. Refsnider, and M.W. Caffee. 2006. Latest Pleistocene advance of alpine glaciers in the southwestern Uinta Mountains, Utah, USA: Evidence for the influence of local moisture sources. *Geology* 34(10): 841-844.
- Nishiizumi, K., M. Imamura, M.W. Caffee, J.R. Southon, R.C. Finkel, J. McAninch. 2007. Absolute calibration of  $^{10}\text{Be}$  AMS standards. *Nuclear Instruments and Methods in Physics Research* 258: 403-413.
- Nishiizumi, K., R.C. Finkel, K.V. Ponganis, T. Graf, C.P. Kohl, and K. Marti. 1996. In situ produced cosmogenic nuclides in GISP2 rock core from Greenland summit. *EOS* 77: OS41B-10.
- Nishiizumi, K., E.L. Winterer, C.P. Kohl, J. Klein, R. Middleton, D. Lal, and J.R. Arnold. 1989. Cosmic ray production rates of  $^{10}\text{Be}$  and  $^{26}\text{Al}$  in quartz from glacially polished rocks. *Journal of Geophysical Research* 94(B12): 17907-17915.
- Otto-Bliesner, B.L., S.J. Marshall, J.T. Overpeck, G.H. Miller, and A. Hu. 2006. Simulating Arctic climate warmth and icefield retreat in the last interglaciation. *Science* 311: 1751-1753.

Overpeck, J.T., B.L. Otto-Bliesner, G.H. Miller, D.R. Muhs, R.B. Alley, and J.T. Kiehl. 2006. Paleoclimatic evidence for future ice-sheet instability and rapid sea level rise. *Science* 311: 1747-1750.

Shackleton, N.J., J. Backman, H. Zimmerman, D.V. Kent, M.A. Hall, D.G. Roberts, D. Schnitker, J.G. Baldauf, A. Desprairies, R. Homrighausen, P. Huddlestun, J.B. Keene, A.J. Kaltenback, K.A.O. Krumsiek, A.C. Morton, J.W. Murray, and J. Westberg-Smith. 1984. Oxygen isotope calibration of the onset of ice-rafting and history of glaciation in the North Atlantic. *Nature* 307(16): 620-623.

Sharma, P. and R. Middleton. 1989. Radiogenic production of  $^{10}\text{Be}$  and  $^{26}\text{Al}$  in uranium and thorium ores: Implications for studying terrestrial samples containing low levels of  $^{10}\text{Be}$  and  $^{26}\text{Al}$ . *Geochimica et Cosmochimica Acta* 53: 709-716.

Stone, J.O., L.K. Fifield, G.L. Allan, and R.G. Cresswell. 1996. Cosmogenic chlorine-36 from calcium spallation. *Geochimica et Cosmochimica Acta* 60: 679-692.

Sugden, D.E., P.G. Knight, N. Livesey, R.D. Lorraains, R.A. Souchez, J.L. Tisons, and J. Jouzel. 1987. Evidence for two zones of debris entrainment beneath the Greenland Ice Sheet. *Nature* 328(16): 238-241.

University of Vermont Cosmogenic Nuclide Laboratory. 2001. Methods for Be and Al Extraction, available online at <http://www.uvm.edu/cosmolab/>.

Weidick, A., H. Oerter, N. Reeh, H.H. Thompson, and L. Thorning. 1990. The recession of the inland ice margin during the Holocene climatic optimum in the Jakobshavn Isfjord area of West Greenland. *Paleogeography, Paleoclimatology, Paleoecology (Global and Planetary Change Section)* 82: 389-399.



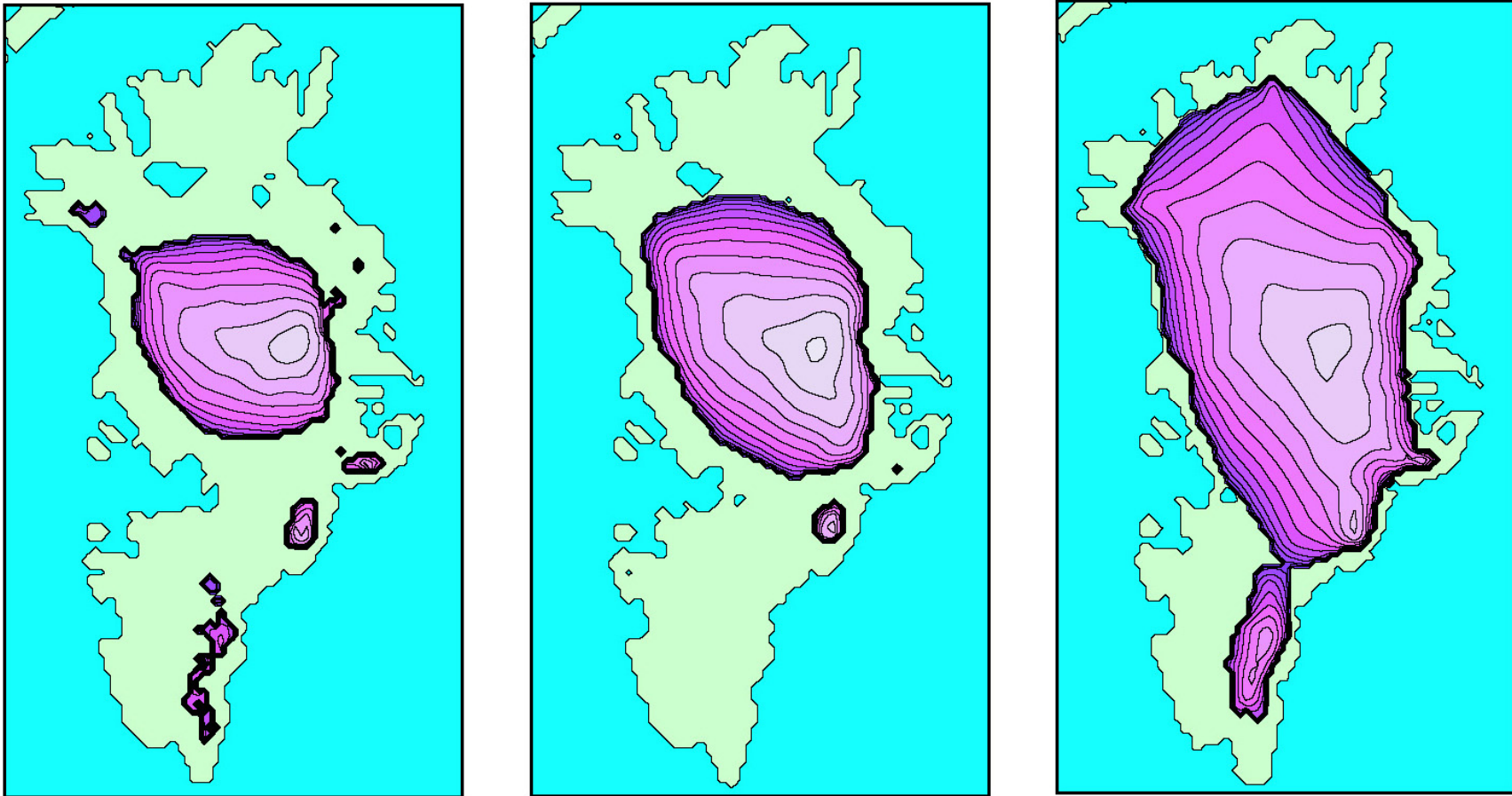


Figure 2a. Modeled ice extent during the Eemian interglacial period (~130 ka) from Cuffey and Marshall (2000). The three images show three possible scenarios, with the middle image being the one most favored by the authors. Even the most conservative model (far right) shows significant melting on the southern peninsula near Kangerlussuaq.

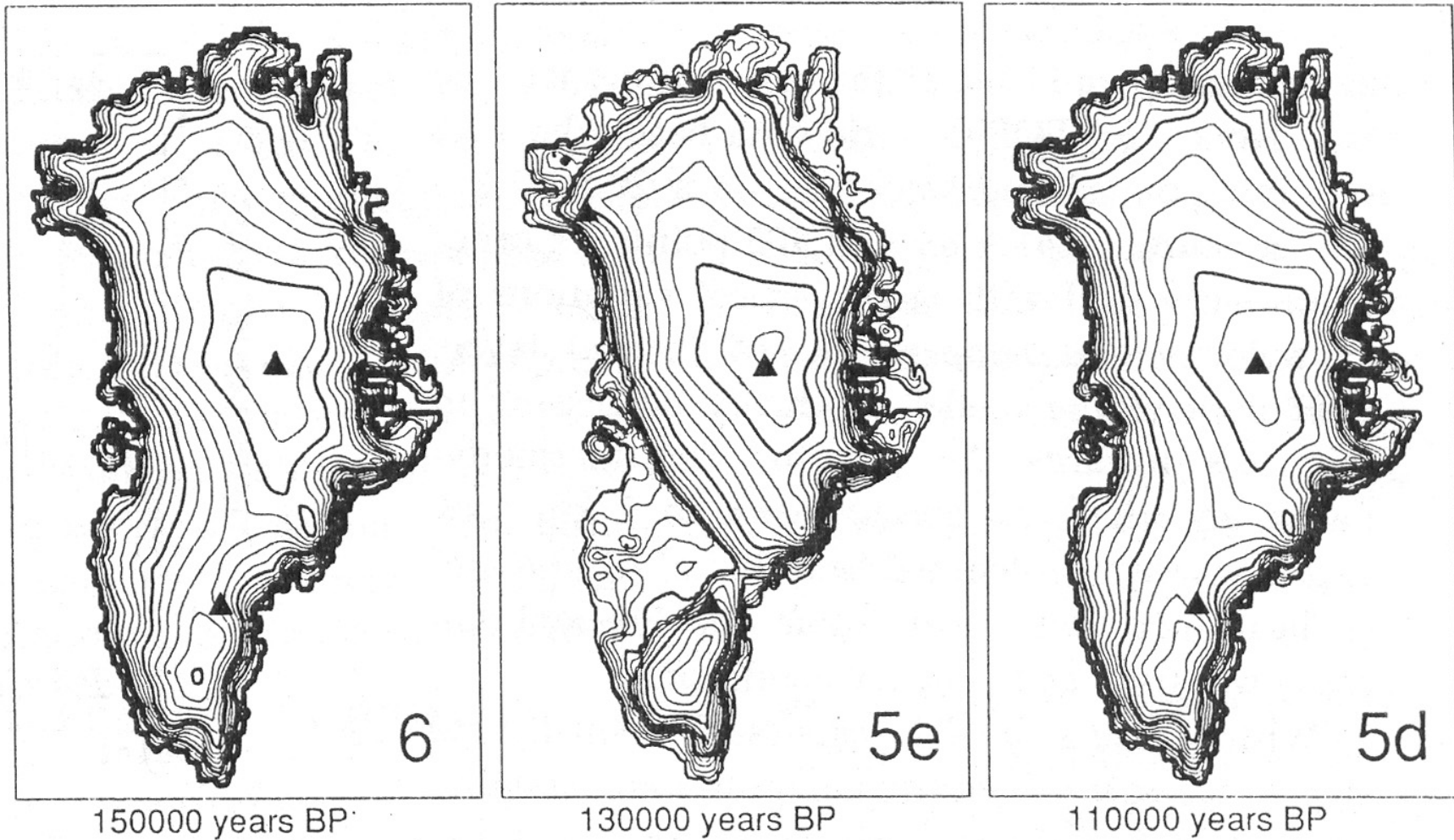


Figure 2b. Modeled ice extent during the Eemian interglacial period (~130 ka) from Letréguilly et al. (1991). The three images show a progression over time at 150 ka (OIS6), 130 ka (OIS 5e), and 110 ka (OIS 5d) respectively. As with Cuffey and Marshall (2000), Letréguilly et al. (1991) suggest that significant melting took place near Kangerlussuaq. Triangles indicate ice core drilling sites (Camp Century, Summit, and Dye 3).



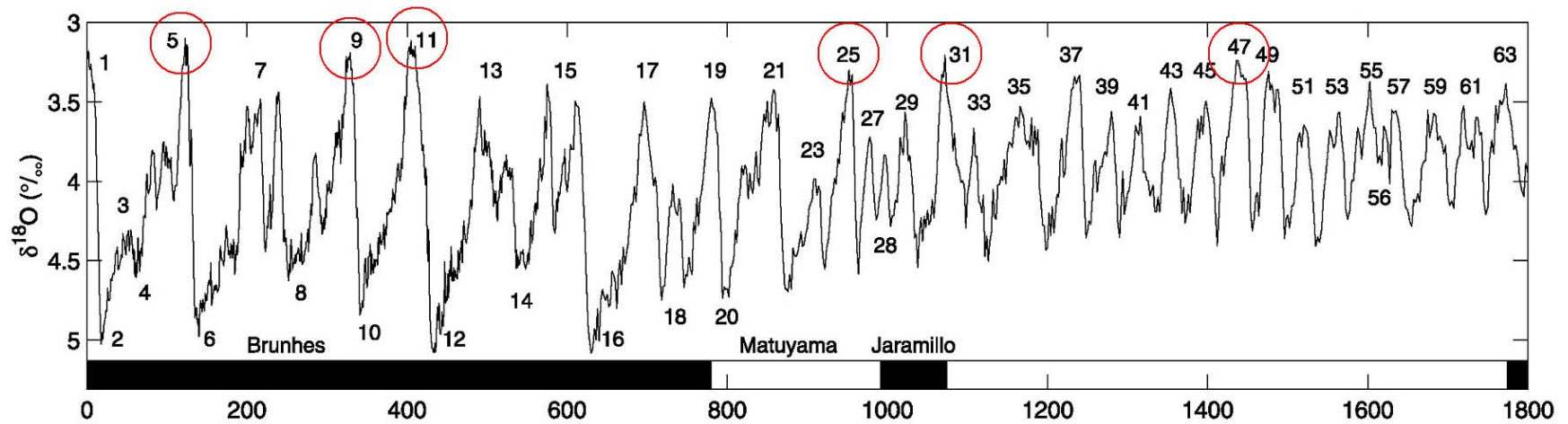


Figure 3. Proxy record for global ice volume derived from oxygen isotope ratios ( $\delta^{18}\text{O}$ ) of benthic foraminifera (Lisiecki and Raymo, 2005). Periods of small ice volume (warm climate) are indicated by low  $\delta^{18}\text{O}$  values at the top of the graph, while periods of large ice volume (cool climate) are indicated by high  $\delta^{18}\text{O}$  values at the bottom of the graph. Time (in ka), along with magnetic reversals, is shown along the horizontal axis. Red circles show OIS stages of smallest global ice volume (less than present day, OIS 1) when the Greenland Ice Sheet likely had minimal extent.

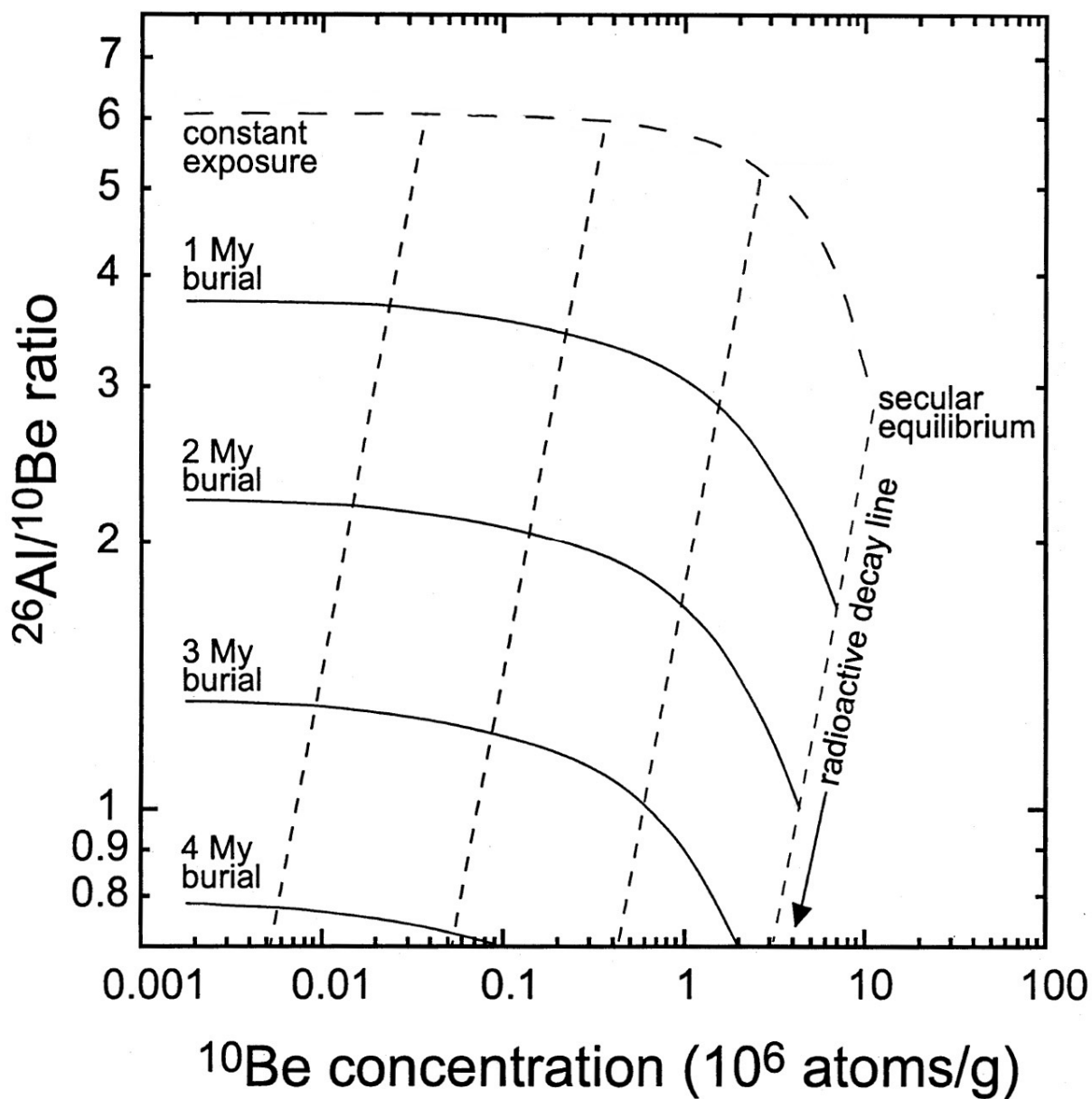


Figure 4. Plot of burial dating paths from the analysis of  $^{26}\text{Al}/^{10}\text{Be}$  in quartz (modified from Granger and Muzikar, 2001). Rock exposed continually on the surface would be expected to follow the dashed “constant exposure” path, the shape of which is determined by the production rates and decay rates of the two TCNs. When subjected to burial, therefore halting TCN production, TCN measurements would move perpendicularly to their original path and towards the burial isochrones.